

Analysis of convective heat transfer coefficient for SG II prototype

Zhiyuan Ren (任志远)*, Jianqiang Zhu (朱健强), Zhigang Liu (刘志刚), and Hongbiao Huang (黄宏彪)

Shanghai Institute of Optics and Fine Mechanics, Chinese Academy of Sciences, Shanghai 201800, China

*Corresponding author: appear2003@126.com

Received April 4, 2012; accepted July 23, 2012; posted online November 23, 2012

The forced convective heat transfer coefficients during the period of thermal recovery for laser slab on the multi-segment amplifiers of SG II is analyzed. We simulate the parameters including coolant gas and the geometry of amplifier with computational fluids dynamics (CFD) method. Based on the simulated results, we attain the optimized parameters such as the flow rate, the temperature and the type of gas, the diameter of inlet jet, the quantity of inlet jet, the distance between the inlet jet and the laser slab, and the spray angle of inlet.

OCIS codes: 140.3580, 140.4480, 140.6810.

doi: 10.3788/COL201210.S21410.

There are some powerful laser systems are built such as the National Ignition Facility (NIF)^[1] at Lawrence Livermore National Laboratory (LLNL) and the Sheng Guang II (SG II)^[2] in China to study inertial confinement fusion (ICF) and high-energy-density science. The multi-segment amplifiers are the main part of the driven laser system. With the requirements for scaling the average power of a solid-state laser, the thermal recovery of multi-segment amplifiers becomes the limiting factor for higher power and cost-effective^[3–5].

The temperature of the components in the amplifier will increase when the flashlamps are fired in multi-segment amplifier. Most of the electrical energy is deposited thermally on the beam tubes, the laser slabs, the blastshield, and so on. The temperature gradient in the Nd:glass slab and among the various components and cavity in the amplifier causes the wave front distortion. To meet requirements of high quality laser beams and high repetition rates, the amplifiers need achieve relatively rapid thermal equilibrium^[6]. The performance of passively-cooled lasers degrades monotonically as shots are accumulated and heat store in the amplifiers. In contrast, with turbulent and slightly chilled gas flowing through the flashlamps and slab cavity, the amplifiers can meet thermal recovery criteria within 3 to 5 h after each shot. Furthermore, with water flowing over the flashlamps, the Omega laser at the University of Rochester attains more rapid thermal recovery in about 20 min after each shot. In view of compact construction of multi-segment in the SG II in China and NIF in LLNL, it is feasible to achieve a accelerated thermal recovery for flashlamped pumped amplifiers with gas. This attracts studies on thermal recovery modeling of multi-segment amplifiers with gas. There are two main parts that need cooling: the flashpump cassette and the cavity of amplifier. The arrangement of single multi-segment amplifiers is shown in Figs. 1 and 2. We have investigated the relationship between the thermal recovery time and the flow rate of coolant gas, the temperature of coolant gas applied to the flash pump cassette and the cavity of amplifier on the NIF in American and SG III in China^[7,8]. The temperature and flow rate of coolant

gas are important parameters in the process of thermal recovery. It is stated that the chilled gas and greater flow rate of coolant gas over the flashlamps can result in a significant decrease of thermal recovery time^[9,10]. But among the components of multi-segment amplifiers, the Nd:glass slab is the most important and more slowly than other components returning to temperature equivalent after shot. It is significant to figure out the relationship between the convective heat transfer coefficient and the overall parameters of the coolant gas and the structure.

In this letter, we analyze and simulate the relationship between the geometry of gas inlet flowing into the slab cavity and the prosperities of coolant gas with the

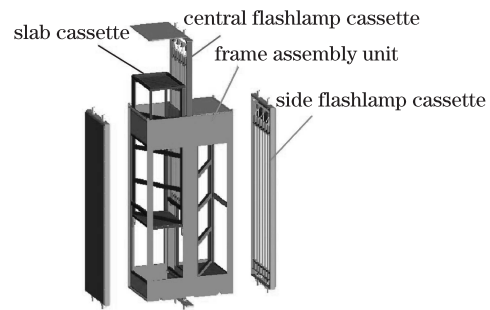


Fig. 1. Structure of multi-segment amplifiers.

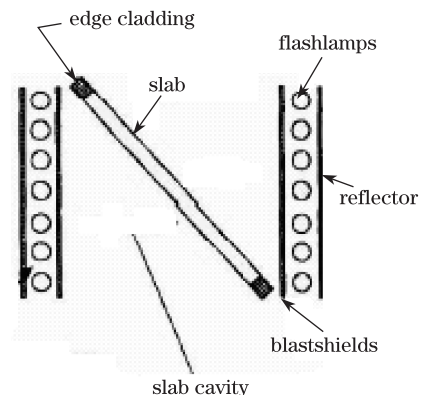


Fig. 2. Main geometry elements in module multi-segment amplifiers.

convective heat transfer coefficient. We have obtained the optimum convective heat transfer coefficient for the geometry construction design with coolant gas inlet and prosperities of coolant gas.

The convective heat transfer is related with many factors as^[11]

$$h = f\left(u, T_s, T_\infty, k, C_p, \rho, \beta, \mu, l, \phi\right), \quad (1)$$

where h is the convective heat transfer coefficient, u is the velocity of the coolant gas, T_s is the temperature of the surface of Nd:glass slab, T_∞ is the temperature of the coolant gas, k is the conductivity of the coolant gas, C_p is the thermal capacity of the coolant gas, ρ is the density of coolant gas, β is the cubical expansion coefficient of the coolant gas, μ is the viscosity of the coolant gas, l is the length of the Nd:glass slab, and ϕ is the relative position coefficient between the Nd:glass slab and coolant gas. There are three factors with the coolant gas which are the flow rate, the temperature, and the type of coolant gas effecting on the heat transfer coefficient respectively; factors with the geometry of amplifiers, which are the diameter of inlet jet, the quantity of inlet jet, and the distance between the inlet jet and the laser slab effecting on the heat transfer coefficient respectively

We consider the Nd:glass slab in the multi-segment amplifiers of finite thickness and width. The control equation and the the boundary conditions are

$$\nabla g \bar{V} = 0, \quad (2)$$

$$\rho_f \bar{V} g \nabla \bar{V} = -\nabla P + \mu_f \nabla^2 \bar{V}, \quad (3)$$

$$\bar{V} g \nabla T_f = \alpha_f \nabla^2 T_f, \quad (4)$$

$$\nabla^2 T_s = 0 \text{ (solid-state slab)}, \quad (5)$$

where \bar{V} , P , and T_f are the velocity vector, pressure, and temperature, respectively; ρ_f , μ_f , and α_f are the mass density, viscosity, and thermal diffusivity of the coolant air, respectively; T_s is the solid temperature.

Subject to the boundary conditions:

$$\begin{aligned} \bar{V} &= 0, -k \frac{\partial T}{\partial y} = h_f(T_f - T_s) \text{ on } y = 0; \\ \bar{V} &\rightarrow \bar{V}_f, T \rightarrow T_f \text{ as } y \rightarrow \infty, \end{aligned} \quad (6)$$

where x and z respectively measure distance along with the Nd:glass slab and y measure distance normal to the Nd:glass slab.

We take 6 main cases of operating conditions. First, we choose N_2 to simulate the flow rates of 0.14, 0.28, 0.42, 0.57, 0.71, and 0.85 $m^3 \cdot min^{-1}$, and find that the best flow rate is 0.42 $m^3 \cdot min^{-1}$. Numerical simulation model is shown in Fig. 3. With the coolant gas temperature of 291 K, inlet jet diameter of 15 mm, inlet jet quantity of 5, and the distance between the Nd:glass slab and inlet jet of 10 mm are shown in Fig. 4. With the air flow rate increasing, the convective heat transfer coefficient increases. But air flow cannot unlimited increase, when the convective heat transfer reaches a level, it will not be developed apparently if we continue to increase coolant gas flow rate. At the same time, the larger flow rate will

create vortices on the surface of Nd:glass slab. When the flow rate is more than 0.42 $m^3 \cdot s^{-1}$, the convective heat transfer coefficient increases slowly.

With the coolant gas flow rate of 0.42 $m^3 \cdot s^{-1}$, inlet jet diameter of 15 mm, inlet jet quantity of 5, and the distance between the Nd:glass slab and inlet jet of 10 mm, we change the temperature of coolant gas (293, 291, 289, 287, 285, and 283 K). The result demonstrates in Fig. 5. As the inlet temperature rises, the convection heat transfer coefficient will be growth linearly. On the considering of chilled gas returning to the room temperature before shot, the temperature of chilled gas below 2 K compared with room temperature, which can ensure the fast thermal recovery for amplifier.

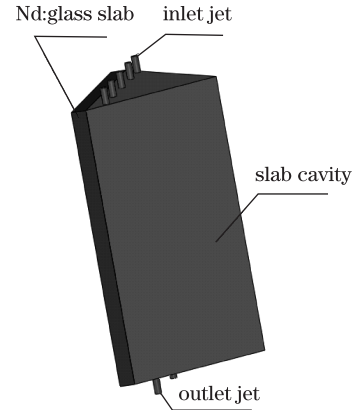


Fig. 3. Schematic of the computational domain for multi-segment amplifier.

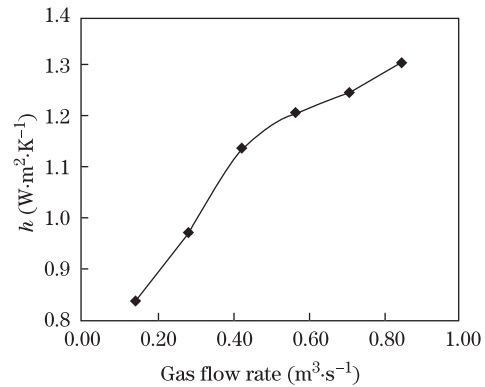


Fig. 4. Convective coefficient h as a function of flow rate.

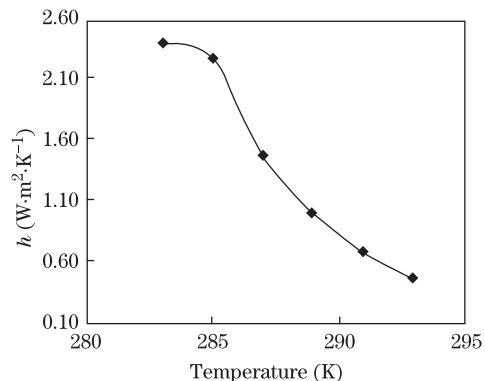


Fig. 5. Convective coefficient h as a function of coolant gas temperature.

With the coolant gas flow rate of $0.42 \text{ m}^3 \cdot \text{s}^{-1}$, the coolant gas temperature of 291 K, inlet jet diameter of 15 mm, inlet jet quantity of 5, and the distance between the Nd:glass slab and inlet jet of 10 mm, we change the type of coolant gas. The result is shown in Fig. 6. It is shown that, the convective heat transfer coefficient is more than others when the coolant gas is hydrogen, and then is the nitrogen. Because the nitrogen is cost effective and safe, we can obtain faster thermal recovery of multi-segment amplifier with nitrogen.

With the coolant air flow rate of $0.42 \text{ m}^3 \cdot \text{s}^{-1}$, the coolant gas temperature of 291 K, inlet jet quantity of 5, and the distance between the Nd:glass slab and inlet jet of 10 mm, we change the diameter of inlet jet. The result is shown in Fig. 7. The convective heat transfer coefficient decrease with the inlet jet diameter increase. The velocity of inlet jet decreases with the inlet jet diameter increases based on the fixed flow rate. And then the thermal boundary layer becomes thicker, the convective heat transfer coefficient decreases. The convective heat transfer coefficient degrades dramatically when the diameter of inlet is larger than 15 mm.

With the coolant air flow rate of $0.42 \text{ m}^3 \cdot \text{s}^{-1}$, the coolant gas temperature of 291 K, inlet jet diameter of 15 mm, and the distance between the Nd:glass slab and inlet jet of 10 mm, we change the quantity of inlet jet. The result is shown in Fig. 8. As the quantity of inlet jet increases from 1 to 8, the convection heat transfer coefficient increases slowly. Because the more quantity of inlet jet, the more fluent of the flow field on the surface of Nd:glass slab. When the quantity of inlet jet

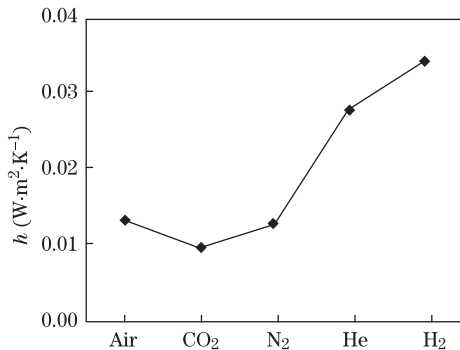


Fig. 6. Convective coefficient h as a function of coolant gas type.

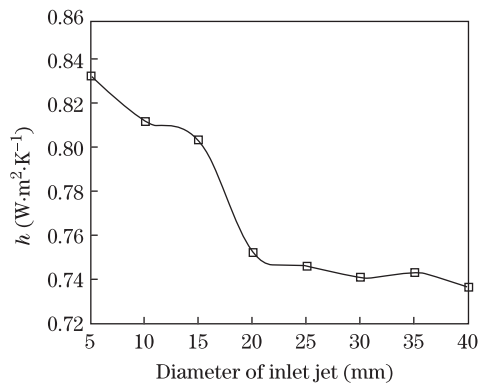


Fig. 7. Convective coefficient h as a function of diameter of inlet jet.

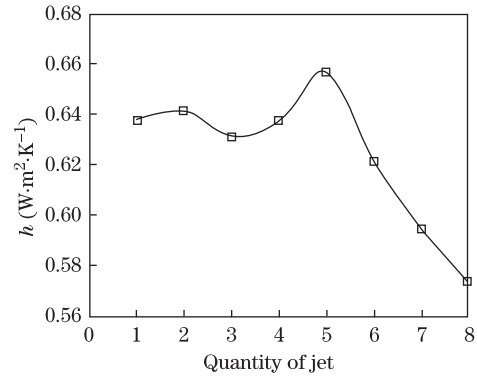


Fig. 8. Convective coefficient h as a function of quantity of inlet jet.



Fig. 9. Convective coefficient h as a function of distance between the Nd:glass slab and inlet jet.

is of 5, continue to increase the quantity of inlet jet, convection heat transfer coefficient will decrease. Because there are vortices on the surface of slab, which degrade the performance of convective heat transfer.

With the coolant air flow rate of $0.42 \text{ m}^3 \cdot \text{s}^{-1}$, the coolant gas temperature of 291 K, inlet jet diameter of 15 mm, and the inlet jet quantity of 5, we change the distance between the slab and inlet jet (1.05, 1.5, 2, 2.5, 5, 10, and 15 mm). The result is shown in Fig. 9. The convective heat transfer decreases with the distance increasing. When the distance between the inlet jet and slab is larger than 10 mm, the convective heat transfer degrades quickly. The thermal boundary layer become thicker when the inlet gas spray over the Nd:glass slab from long distance.

In conclusion, based on the analysis the factors of convective heat transfer coefficient of the multi-segment amplifier, we obtain operating conditions for the 6 main cases to numerical simulation, which is the flow rate of coolant gas, the temperature of coolant gas, the type of coolant gas, the diameter of inlet jet, the quantity of inlet jet, and the distance between Nd:glass slab and inlet jet. In this letter, we attain the optimum design for the inlet gas and geometry of inlet jet for the multi-segment amplifier in SG II. With the coolant air flow rate of $0.42 \text{ m}^3 \cdot \text{s}^{-1}$, the coolant gas temperature 291 K, inlet jet diameter of 15 mm, the inlet jet quantity of 5, and the distance between the slab and inlet jet of 10 mm, the multi-segment amplifier can reach thermal equilibrium quickly. This can be applied to the optimum cooling design for solid-state laser.

References

1. E. Gerstner, *Nature* **446**, 16 (2007).
2. P. Lacovara, H. Choi, C. Wang, R. Aggarwal, and T. Fan, *Opt. Lett.* **16**, 1089 (1991).
3. H. Yu, W. Zheng, C. Wang, J. Tang, S. He, Y. Liu, H. Zhou, D. Lin, X. Jiang, and L. Guo, *Opt. Eng.* **42**, 725 (2003).
4. H. T. Powell, A. C. Erlandson, K. S. Jancaitis, and J. E. Murray, *Proc. SPIE* **1277**, 103 (1990).
5. J. A. Horvath, *Proc. SPIE* **3047**, 148 (1997).
6. M. Rotter, K. Jancaitis, C. Marshall, L. Zapata, A. Erlandson, G. LeTouze, and S. Seznec, *Proc. SPIE* **3492**, 638 (1999).
7. G. Albrecht, S. Sutton, E. George, W. Sooy, and W. Krupke, *Laser Particle Beams* **16**, 605 (1998).
8. M. L. Spaeth, K. R. Manes, C. C. Widmayer, W. H. Williams, P. K. Whitman, M. A. Hennesian, I. F. Stowers, and J. Honig, *Opt. Eng.* **43**, 2854 (2004).
9. A. Li, X. Jiang, J. Sun, L. Wang, Z. Li, and L. Liu, *Appl. Opt.* **51**, 356 (2012).
10. H. Yu, W. Zheng, C. Wang, S. He, J. Tang, Y. Liu, and Y. C. Yu, *Opt. Eng.* **40**, 126 (2001).
11. J. Wang, J. Min, and Y. Song, *Appl. Thermal Eng.* **26**, 549 (2006).